



## Developing Performance Levels for Concrete Bridge Bents with a Focus on the Joint Region

Bahrani, M.K.<sup>1\*</sup>, Nooralizadeh, A.<sup>2</sup>, Sharifi, M.<sup>1</sup> and Karami, N.<sup>2</sup>

<sup>1</sup> Assistant Professor, Department of Civil Engineering, University of Qom, Qom, Iran.

<sup>2</sup> Ph.D. Candidate, Department of Civil Engineering, University of Qom, Qom, Iran.

© University of Tehran 2021

Received: 08 Nov. 2020;

Revised: 15 Jun 2021;

Accepted: 12 Jul. 2021

**ABSTRACT:** Bridges are critical highway structures, and damage to them can result in the loss of vital lifelines. Many bridges reaching the end of their expected lifespans should have their seismic performance evaluated immediately. The study utilized a 1/3 scale model of two-column bridge bents developed within the last 20 years that split from the deck under cyclic loads. The purpose is to investigate seismic performance and define performance levels utilizing experimental observation. The damage estimates from previous studies for each performance level were reviewed and, where necessary, revised. Damage and performance levels for joints were estimated differently than for other components such as cap beams and columns, according to the findings. The present study proposes new performance levels including joint damage. The overall seismic performance of the concrete bridge bents revealed that the anticipated mechanisms did not occur, but that flexural hinges formed in the joint region rather than in the columns, as required by current codes.

**Keywords:** Concrete Pier, Cyclic Loading, Damage, Performance Level, Seismic Performance.

### 1. Introduction

Critical infrastructures are essential for post-earthquake maintenance to facilitate response; therefore, they must be available for immediate use after an earthquake (Abudallah Habib et al., 2020; Samadi et al., 2021). Seismic criteria have been stated in the design regulations and seismic design philosophy (AASHTO, 2011; Ghassemieh et al., 2018), and several researchers have studied the seismic and strengthening performance of bridges built to these standards. They proposed various ways to improve the behavior of concrete piers on

bridges in response to earthquakes, including the use of divergent bracing (Rahnavard et al., 2017; Rahnavard and Hassanipour, 2015), non-buckling bracing (Naghavi et al., 2019; Rahnavard et al., 2018), bracing concrete-steel composite walls (Rahnavard et al., 2016), seismic insulators (Radkia et al., 2018, 2019; Rahnavard and Thomas, 2019) and concrete-steel composite connections (Rahnavard et al., 2017).

Extensive research has also been conducted to develop quantitative and qualitative definitions, as well as to determine damage levels for concrete

\* Corresponding author E-mail: mkbahrani@ut.ac.ir

frames. Hose et al. (2000) conducted one of the most important studies on the levels of damage to bridge concrete bents. They reviewed previous laboratory studies to determine damage levels as well as performance levels, and they proposed design criteria for use in bridges.

Bahrani et al. (2010, 2017) conducted a series of laboratory investigations at 1/3 scale for multi-column concrete bridge bents subjected to lateral cyclic loads to identify damage and failure modes such as joint failure and longitudinal reinforcement slide at joints. Their findings revealed that the energy dissipation capacity and pinching in the cyclic response had a substantial impact on these damage and failure types. The authors analyzed the members' performance levels and proposed three improvement plans: lowering column shear demand by reducing the effective cross-section of the bars; transverse external post-tensioning; and transverse and longitudinal external post-tensioning in the cap-beam.

Hasaballa et al. (2011) investigated the seismic performance of concrete beam-column exterior joints reinforced with Fiber Reinforced Polymer (FRP) and Glass Fiber Reinforced Polymer (GFRP) rebars. They focused on four laboratory specimens with T-shaped connections and discovered that beam-column connections retrofitted with GFRP rebars and stirrups spared considerable damage under seismic loading.

Vecchio et al. (2014) conducted a series of laboratory studies on beam-column joints retrofitted externally with FRP. They investigated the behavior of non-transverse reinforcement (confinement) of joints that did not comply with current seismic codes as well as the effect of FRP as a strengthening method under constant axial loading and transverse cyclic loading in the as-built and strengthened specimens.

Tukiar et al. (2014) investigated the seismic performance of a beam-column precast corner joint with corbels subjected to up to 1.5 percent drift under lateral

loading. They investigated the seismic performance of exterior reinforced concrete beam-column joints reinforced using various techniques. According to the findings, the proposed strengthening methods increased the seismic capacity of the joints and steel jackets, consequently increasing their load-bearing capacity and ductility.

Lowes and Moehle (1999) conducted an experimental study on beam-column T-joints to investigate common defects in bridges built between 1950 and 1970, such as insufficient column reinforcement development length, a lack of transverse reinforcement in the joint regions (spacing equal to 20 times the diameter of the reinforcement), and cutting 50 percent of the lower reinforcement of the beams near the joint. They also investigated the behavior of joints that had been improved with RC covers. The findings demonstrated that this method was effective in increasing the ductility capacity and shear strength of the joints.

KhanMohammadi et al. (2016) investigated 1/4 scale two-column concrete bridge piers. In primary studies, they discovered significant joint damage and proposed a retrofitting method for the joint. The results showed that the retrofitted specimens had no damage in the joint region and that plastic hinges formed at the ends of both columns in accordance with the mechanism specified in seismic codes.

Bilah et al. (2013) investigated the vulnerability of multi-column bridge bents in near-fault and far-field ground motion. They studied the effects of different retrofitting methods on bridges (steel jackets, concrete jackets, Carbon FRP (CFRP) jackets, and Engineered Cement Composite (ECC) jackets). The ECC and CFRP jackets reduced vulnerability effectively.

Patel et al. (2013) studied the exterior beam-column joints of RC and SFRC structures subjected to cyclic loading in order to reduce confinement reinforcement at the connection zone. Six exterior beam-

column joints were tested at 1/3 scale under cyclic loading. 1.5 percent steel fibers were used in the SFRC beam-column joint. Their findings revealed that the SFRC beam-column joint performed well and that joint behavior improved. Furthermore, the findings indicated that reducing the number of stirrups in a properly reinforced SFRC joint could be considered as an alternative solution to avoid retrofitting the connection zone.

Under cyclic loading, Kaliluthin and Kothandaraman (2017) tested exterior beam-column joint specimens at 1/3 scale using the core strengthening technique. The first set of specimens was detailed as ordinary moment-resisting frames, while the second set was detailed as special moment-resisting frames. The third set followed reinforcement detailing with a new type of reinforcement known as "core reinforcement". According to the experimental results, the strengthened joint performed better in terms of bearing capacity, energy absorption, stiffness coefficient, and ductility. It was discovered that the beam-column exterior joint models with core reinforcement provided adequate stiffness and ductility, and that the stiffness did not decrease significantly when compared to the other joint types.

Deng et al. (2015) studied damaged bridge piers that had been repaired post-earthquake using steel tubes and FRP. The behavior was investigated using both experimental and Finite Element (FE) approaches. Steel tubes, Basalt Fiber Reinforced Polymer (BFRP), or CFRP were used to repair the three damaged circular RC piers. The repaired piers had hysteresis curves similar to the original specimens, and all three repair methods recovered the seismic performance of the damaged earthquake piers, according to FE analysis and experimental observation.

The findings of the preceding research indicate that the seismic cyclic loading performance of a large number of older bridges designed in accordance with codes at the time of construction should be

investigated. The current study performed laboratory testing on one-span concrete piers with two concrete bents at 1/3 scale that were designed in accordance with code in the previous 20 years.

Using experimental observation, the current study investigates seismic performance and defined performance levels. Based on the observations, the types of damage associated with each performance level are defined, and qualitative and quantitative definitions are developed. Furthermore, the seismic behavior and performance of the specimen's components are investigated.

## 2. Test Program

### 2.1. Specifications of Specimens

Initially, two as-built one-span specimens (SP-80 and SP-90) were investigated. In the 1980s and 1990s, these specimens were built in accordance with conventional design and construction regulations in Iran. The addition of transverse reinforcement in the joint region is the most significant difference between these two periods.

The specimens were generated at a scale of one-third. The column's arrangement and number of longitudinal reinforcements were the same as in existing codes, and it had full-column cross-section symmetry. Figures 1a and 1b depict the geometry and basic details of existing bridges as well as experimental specimens SP-80 and SP-90.

Tables 1 and 2 show the mechanical properties of the materials used, including the concrete compressive strength in the cap beam and columns, as well as the reinforcement properties. The ratio of longitudinal and transverse reinforcement, joint area details, and cross-section dimensions in these specimens were based on the mean of six bridges with roughly similar conditions (Table 3). Figure 1 depicts the specimen layout and cross-section.

**Table 1.** Compressive strength of concrete in MPa (  $fc'$  )

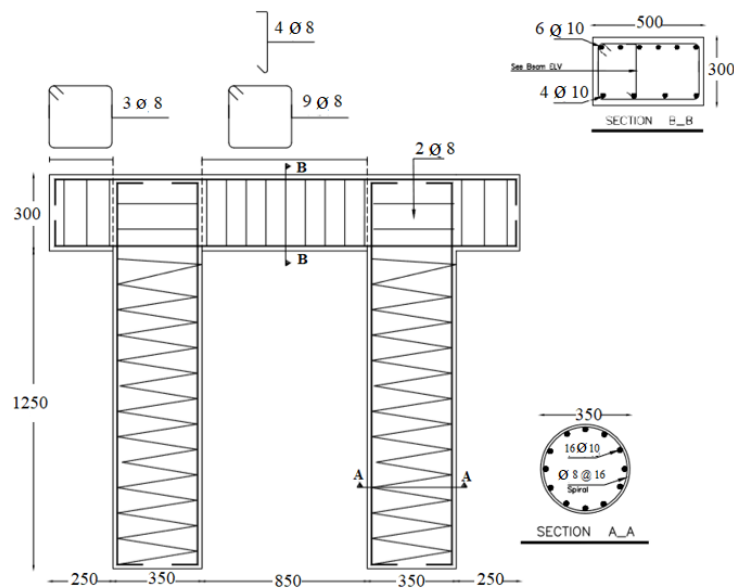
| Cap beam | Column |
|----------|--------|
| 42.1     | 41.7   |

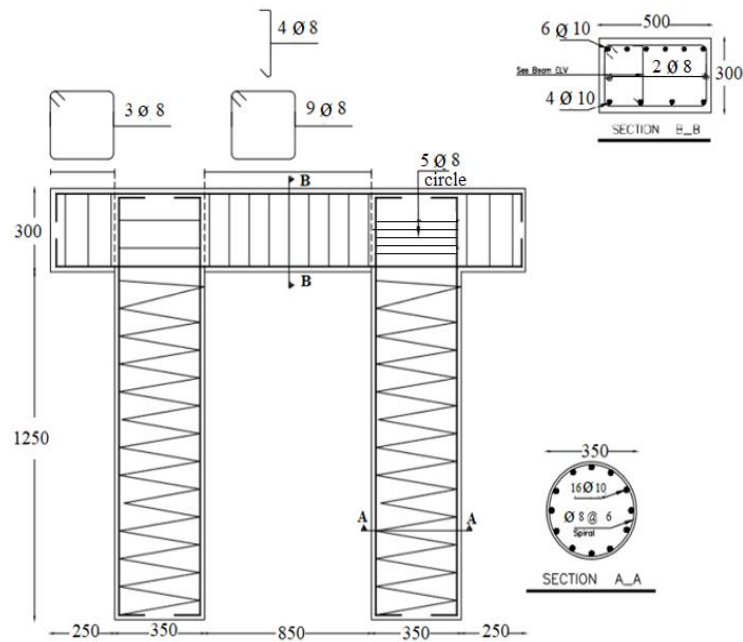
**Table 2.** Mechanical properties of the longitudinal and transverse reinforcement used in the specimen

| Reinforcement type | Yield stress (MPa) | Ultimate stress (MPa) | Ultimate strain (%) |
|--------------------|--------------------|-----------------------|---------------------|
| longitudinal       | 511.4              | 653.2                 | 12.56               |
| transverse         | 365.4              | 540.8                 | 12.34               |

**Table 3.** Bridges information for experimental specimen design

| Average                    | Saveh   | Kesma    | Azadegan | Mohajeran | Aramene  | Molasadra | Kashani  | Unit   | Specifications                           |
|----------------------------|---------|----------|----------|-----------|----------|-----------|----------|--------|--|
| 18.4                       | 22.5    | 16       | 20.5     | 19        | 19       | 15.5      | 16.5     | m      | Bridge span                              |
| <b>Column information</b>  |         |          |          |           |          |           |          |        |  |
| 1329                       | 1400    | 1200     | 1100     | 2000      | 1200     | 1200      | 1200     | mm     | Section diameter                         |
| 7086                       | 10000   | 4500     | 7000     | 7600      | 6800     | 7000      | 6700     | mm     | Height                                   |
| 4814                       | 5000    | 4000     | 4000     | 5200      | 6500     | 5000      | 4000     | mm     | Column spacing                           |
|                            | 25T25   | 18T28    | 32T32    | 30T28     | 34T25    | 16T32     | 22T26    |        | Longitudinal reinforcement               |
| 1.27                       | 0.8     | 0.98     | 2.71     | 0.78      | 1.48     | 1.14      | 1.03     | %      | Percentage                               |
|                            | T16@10  | T14@50   | T12@15   | T12@75    | T12@65   | T12@125   | T16@70   |        | Transverse reinforcement of hinge region |
|                            | spiral  | spiral   | spiral   | spiral    | spiral   | spiral    | hoop     | spiral | Type                                     |
| 0.42                       | 1.44    | 0.26     | 0.69     | 0.08      | 0.14     | 0.08      | 0.24     | %      | Percentage                               |
|                            | T12@100 | T14@100  | T12@200  | T12@100   | T12@200  | T12@200   | T10@150  |        | Shear reinforcement                      |
| 0.06                       | 0.08    | 0.13     | 0.05     | 0.06      | 0.05     | 0.05      | 0.04     | %      | Percentage                               |
| <b>Capbeam information</b> |         |          |          |           |          |           |          |        |  |
| 1058                       |         | 1400     | 1200     | 1200      | 550      | 1000      | 1000     | mm     | Section width                            |
| 1717                       |         | 1600     | 1600     | 2100      | 1500     | 1750      | 1750     | mm     | Cross section width                      |
|                            |         | 8T28     | 12T25    | 12T32     | 8T25     | 12T25     | 11T28    |        | Top reinforcement                        |
| 0.35                       |         | 0.22     | 0.31     | 0.38      | 0.48     | 0.34      | 0.39     | %      | Percentage                               |
|                            |         | 8T22     | 12T20    | 8T28      | 10T25    | 12T25     | 7T28     |        | Down reinforcement                       |
|                            |         | 0.14     | 0.20     | 0.20      | 0.59     | 0.34      | 0.25     | %      | Percentage                               |
|                            |         | 4T12@250 | 6T14@150 | 6T14@150  | 6T12@150 | 6T12@120  | 6T10@200 |        | Transverse reinforcement                 |
| 0.26                       |         | 0.11     | 0.38     | 0.29      | 0.3      | 0.32      | 0.13     | %      | Percentage                               |
| <b>Joint information</b>   |         |          |          |           |          |           |          |        |  |
|                            |         |          |          | 400       | 500      | 0         | 600      | mm     | Confining reinforcement                  |
|                            |         |          |          | 12        | 12       | 0         | 16       | mm     | Applied length                           |
|                            |         |          |          | 75        | 65       | 125       | 70       | mm     | Diameter                                 |
| 0.46                       |         |          |          | 0.3       | 0.58     | 0.00      | 0.96     | %      | Percentage                               |
| 638                        |         |          |          | 400       | 450      | 850       | 850      | mm     | Anchorage length of column reinforcement |
| 475                        |         |          |          | 400       | 400      | 500       | 600      | mm     | hook length of column reinforcement      |

**(a) Details of the laboratory specimen Sp-80**



(b) Details of the laboratory specimen Sp-90

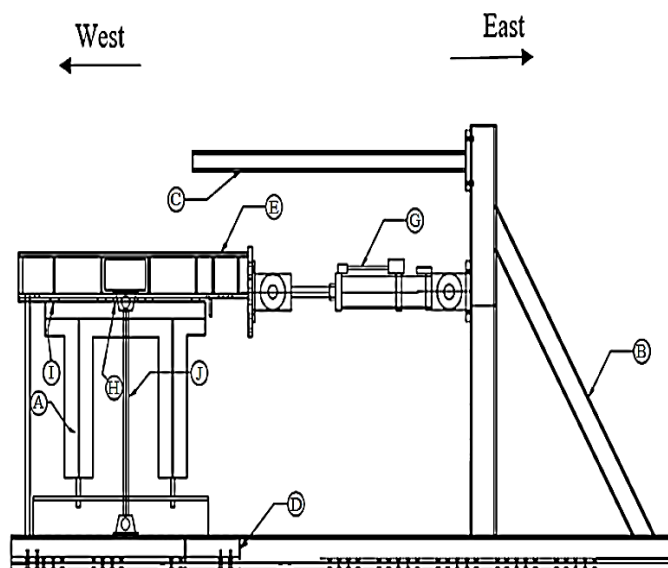
Fig. 1. Details of the studied bridge and experimental specimens

### 2.2. Test Set-up

Figure 2 shows the components used to install and adjust the specimens as well as provide a rigid base. To achieve the desired hinged support conditions, two high-strength bolts were used at the column's end to connect the concrete bents to the rigid steel beam (Figure 3). Figures 4-7 show the locations of the gauges.

Gravity loading was applied using a cross-shaped steel beam (Figure 8). Figure 9 depicts the overall test setup. The steel beam, which had a joint at each end, was installed to control the jack force. The

distribution of gravity load caused by neoprene at regular intervals between the steel cross-beam and the cap beam. The lateral load was transmitted using a steel shear key (Figure 9). The gravity load was applied using a steel beam installed by a control force jack and a steel element with a joint at both ends. The neoprene causes the gravity load distribution, and is arranged at regular intervals between the steel cross beam and the cap beam. The lateral load was transmitted using a steel shear key (Figure 10).



- A: Bridge pier bent specimen
- B: Steel frame for shear force jack and load cell installation
- C: Reliable holder for Jack
- D: Steel beam for specimen and rigid base connection
- E: Cross-shape beam for gravity load applying
- G: Cyclic loading jack
- H: Steel shear key for transmission shear load
- I: Neoprene plane for gravity load applying
- J: Hinge ends steel element



**Fig. 2.** Set up details



**Fig. 3.** High strength bars



**Fig. 4.** Connecting the specimen to a steel beam (rigid floor)



Fig. 5. Displacement control of the end of the cap beam relative to the rigid floor



Fig. 6. Possible slip control of the specimen relative to the steel beam



Fig. 7. Out of plane deformation control (probable rotation control)



**Fig. 8.** Applying gravity load



**Fig. 9.** Specimen set up



**Fig. 10.** Steel shear key between cap beam and cross beam



### 2.3. Load Pattern

ATC24 (ATC24, 1992) was followed when applying the lateral load. Yield displacement was estimated using observations from the first test as well as early software modeling. The cycles continued until the yield coefficients shifted to the end of testing. Figure 11 represents the lateral load pattern.

## 3. Results and Observations

### 3.1. Hysteresis Curves

The response hysteresis curve of the two specimens is presented in Figures 12 and 13. The ultimate failure mechanism is presented in Figures 14 and 15. In all displacements, loss of strength was

observed to follow a similar trend. Throughout the loading process, the loss-of-strength condition in SP-90 was slightly better (less than 5 percent at the same displacement). According to the hysteresis curves, the maximum force applied to the SP-80 and SP-90 was approximately 100 kN, and the maximum force applied in the elastic state occurred at a displacement of 15 mm. As a result, the small change in the connection zone had little effect on the bent strength and stiffness, as expected. The purpose of increasing the number of stirrups in the joint region was to improve the seismic behavior through modification of the failure mechanism by transmitting the hinges to the tops of the columns.

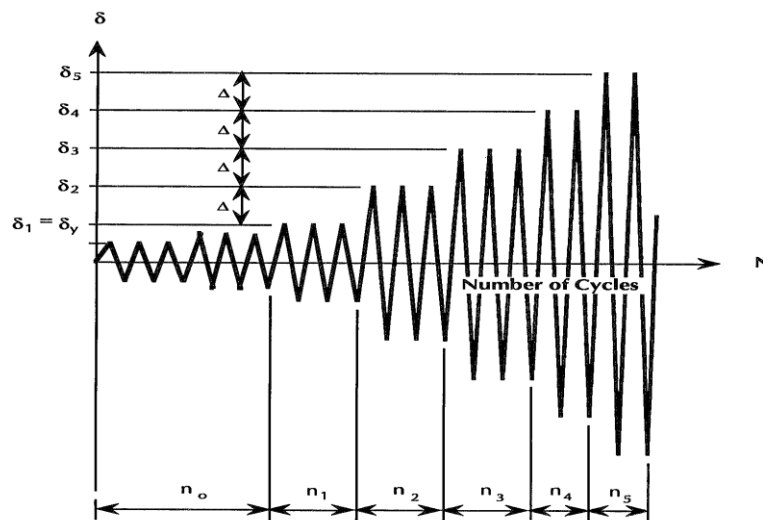


Fig. 11. Quasi-static loading pattern in ATC-24 (ATC24, 1992)

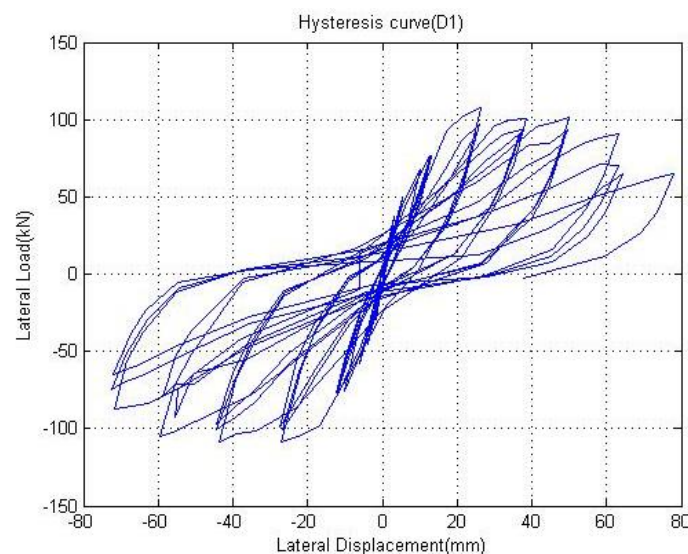
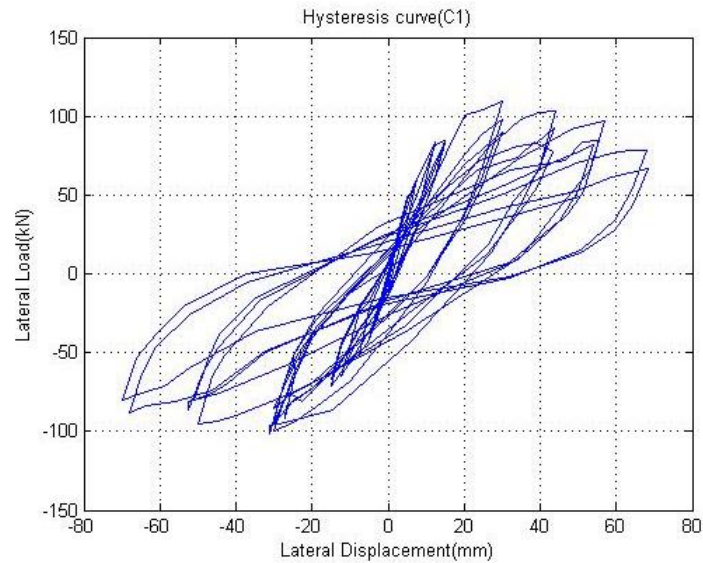


Fig. 12. Hysteresis curve of SP-80



**Fig. 13.** Hysteresis curve of SP-90



**Fig. 14.** Ultimate damage mechanism for SP-80



**Fig. 15.** Ultimate damage mechanism for SP-90

### 3.2. Damage Development

The results of experimental studies were compared to those of the current study to develop new performance levels. Table 4 shows the qualitative and quantitative definitions of joint performance levels. This classification distinguishes five

performance levels: cracking (I), yielding (II), onset of local mechanism (III), completion of local mechanism (IV), and loss of strength (V). Table 4 shows the qualitative damage types associated with each performance level.

Since in this article, an attempt has been

made to develop quantitative and qualitative definitions of performance levels and damages, with special attention to the connection area, during the test, both specimen must inspect the connection conditions with the head and column beam conditions. Given the improved structural details mentioned for the 1990s example,

generalize to determine whether damage was transferred from the connection to other components in order to approach the appropriate seismic failure mechanism. It is necessary to suggest for the column and cap beam as shown in Table 4 for connection in Tables 5-6.

**Table 4.** Proposed performance levels for joint

| Level | Performance                   | Qualitative description   | Quantitative description   |
|-------|-------------------------------|---|--|
| I     | Cracking                      | Diagonal capillary crack in joint; cold joint capillary crack (strain penetration)  | Cold joint crack less than 1 mm in width; extension of diagonal crack to 2/3 width of cross-section                                |
| II    | Yielding                      | Vertical crack in joint region along column longitudinal reinforcement  | Cold joint crack of over 1 mm in width; diagonal crack of over 0.5 mm in width   |
| III   | Onset of local mechanism      | Reinforcement pullout (slip); extension of diagonal crack (corner to corner); concrete spalling of joint surfaces   | Cold joint crack exceeds 3 mm in width; diagonal crack exceeds 1 mm in width; vertical crack exceeds 1 mm in width                 |
| IV    | Completion of local mechanism | Concrete spalling in joint region; objective view of column longitudinal reinforcement or stirrups through cold joint   | Cold joint crack exceeds 5 mm in width; diagonal crack exceeds 2 mm in width   |
| V     | Loss of strength              | Concrete spalling on upper surface of joint; inadequate anchorage of longitudinal reinforcement in joint region (full slip or stirrup opening); visible permanent deformation in joint region | Core crack in joint exceeds 2 mm; insufficient anchorage of longitudinal reinforcement; fracture of transverse joint reinforcement |

**Table 5.** Define major damages and assign them to performance levels for the column

| Level | Performance   |
|-------|---|
| I     | Bending capillary crack   |
| II    | Cracking less than 1 mm<br>Opening of cracks (1 to 2 mm)<br>Full depth cracking   |
| III   | Expansion of the diagonal crack<br>Concrete spalling (more than 1/10 section depth)<br>Increase crack width more than 2 mm      |
| IV    | The expansion was more than 1.2 section depth<br>Diagonal cracking more than 2/3 section depth<br>visible permanent deformation |
| V     | Reinforcement buckling or failure<br>Cracking of concrete core more than 2 mm   |

**Table 6.** Define major damages and assign them to performance levels for the cap beam

| Level | Performance   |
|-------|---|
| I     | Capillary crack - positive bending<br>Capillary crack - negative bending  |
| II    | Cracking less than 1 mm<br>Opening of cracks (1 to 2 mm)  |
| III   | Expansion of the diagonal crack<br>Sliding column reinforcements<br>Expansion of concrete spalling (more than 1/10 section depth)   |
| IV    | Diagonal cracking more than 2/3 section depth<br>Expansion of concrete spalling (more than 2/3 section depth)<br>Increase crack width more than 2 mm<br>Visible permanent deformation |
| V     | Reinforcement buckling or failure<br>Shear and slip failure   |

The testing results were then compared to the performance criteria in Table 4. The major types of damage sustained by SP-80, which affected the majority of the bridge components, were identified. Level I capillary cracks were observed at all five levels, primarily in flexural members such as the cap beam, and were caused by bending. Such cracks were observed less often in the joint region.

Diagonal cracks generally occur in the joint region due to shear. Capillary cracks in a cold joint, on the other hand, indicate longitudinal column reinforcement slippage in the joint region. Slippage was a major issue in the bents studied in terms of seismic behavior. Cold joint cracking was added to performance level I because it was discovered early on to be caused by strain penetration.

A crack opening exceeding 1 mm, particularly for the cold joint crack, is a criterion at performance level II. According to Bahrani et al. (2010), the 1-mm cold joint crack opening is related to slippage and results in reinforcement yielding. However, the current study found that the reinforcement did not yield and no slippage was observed for a cold joint crack opening. Furthermore, at this performance level, the diagonal crack width criterion was set at 0.5 mm. Furthermore, cold joint cracking was classified as occurring in the joint rather than the column.

In performance level II, Bahrani et al. (2010) reported a cold joint crack width greater than 3 mm as a sign of slippage. Their findings, as well as those of other researchers, have resulted in the inclusion of slippage of longitudinal reinforcement of the column in the joint region at this level of performance. However, because this was not observed in the current experimental study, this item has been classified as performing at the third level.

Items classified as performance level IV include an increase in crack width of more than 2 mm, a cold joint crack opening greater than 5 mm, and concrete spalling that extends up to 50% of the width. These

items will increase nonlinear behavior, which will result in a significant increase in strain.

The lateral load displacement hysteresis curve clearly shows performance level V, loss of strength. At this level of performance, many behaviors can be observed, but one of the most important is permanent deformation. At the end of the experiment, such deformation was clearly visible due to shear strain in the joint region. Furthermore, cracks in the concrete core that were wider than 2 mm were indicators of deterioration. As an indicator of performance level V, severe slippage of the column longitudinal reinforcements was added to this level. Table 7 depicts the various types of major damage and their joint performance levels.

### 3.2.1. Specimen SP-80

As shown in Table 7, all damages observed in the components and joint region have been described in terms of relative displacement. The first cracks were discovered in the joint region at a relative displacement of 0.73 percent (capillary cracks and diagonal cracks of less than 2.3 mm in width). A diagonal crack exceeding 0.5 mm occurred at the right joint at a relative displacement of 1.83 percent. Strain penetration caused a crack opening greater than 1 mm at the left cold joint. At a relative displacement of 2.73 percent in the joint region, the diagonal cracks extended to more than 1 mm (Figures 16-19).



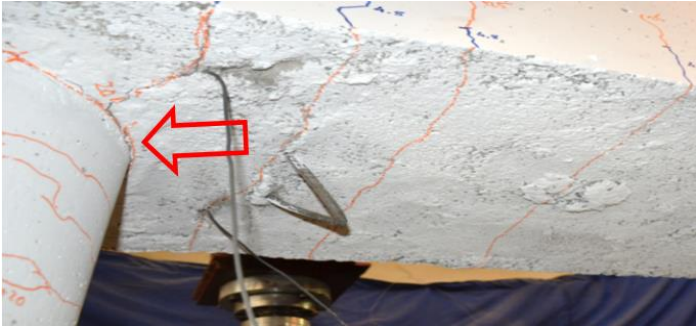

### 3.2.2. Specimen SP-90

Table 8 shows the progression of damage in the joints of the SP-80 specimen in terms of relative displacement, which is illustrated in Figures 20-24. At a relative displacement of 0.43 percent, the first crack appeared (capillary and diagonal cracks of less than 2.3 mm in width). A cold joint capillary crack appeared in the interior surface of the left connection at 0.92 percent displacement, and a cold joint capillary crack appeared in the exterior surface of the eastern joint at 0.92 percent displacement.





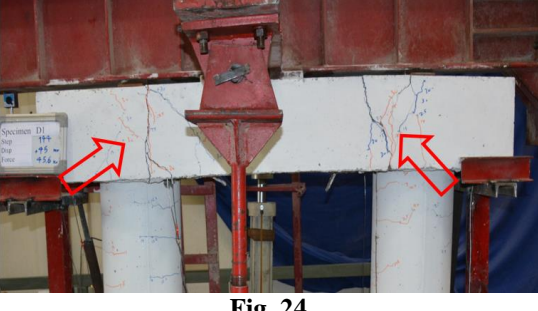
Diagonal cracks of greater than 0.5 mm were observed at a relative displacement of 1.82% in the left joint. At this displacement, the cold joint crack opened wider than 1

mm. At a relative displacement of 3.64%, the width of the cracks in the eastern and left joints exceeded 2 mm.

**Table 7.** Damage development in joint region (red denotes freight loads and blue denotes return loads)

| Order | Damage type  | Lateral displacement (%) | Figure   |
|-------|--|--------------------------|--|
| 1     | Capillary cracks and diagonal cracks of less than 2.3 mm in width  | 0.73                     |  <p><b>Fig. 16.</b></p>  |
| 2     | Diagonal crack exceeding 0.5 mm at eastern joint; diagonal crack exceeding 1 mm in width at left cold joint crack opening caused by strain penetration | 1.83                     |  <p><b>Fig. 17.</b></p>  <p><b>Fig. 18.</b></p> |
| 3     | Extension of diagonal cracks exceeding 1 mm in length in joint region  | 2.73                     |  <p><b>Fig. 19.</b></p>  |

**Table 8.** Damage development at joints

| Order | Damage type  | Lateral displacement (%) | Figure  |
|-------|--|--------------------------|---|
| 1     | Capillary crack and diagonal crack of less than 2.3 mm in width. | 0.43                     |  <p><b>Fig. 20.</b></p>   |
| 2     | Cold joint capillary crack in left joint                         | 0.92                     |  <p><b>Fig. 21.</b></p>   |
| 3     | Cold joint capillary crack in eastern joint                      | 0.93                     |  <p><b>Fig. 22.</b></p>  |
| 4     | Diagonal cracks exceeding 0.5 mm observed in left joint          | 1.82                     |  <p><b>Fig. 23.</b></p> |
| 5     | Crack width in eastern and left joints exceeded 2 mm.            | 3.64                     |  <p><b>Fig. 24.</b></p> |

## 4. Analysis of Results

The performance of the specimens tested was evaluated, compared, and analyzed. The performance of the components, as well as the relative displacements corresponding to their performance levels, have been quantitatively compared and evaluated.

### 4.1. Qualitative and Quantitative Indices

The quantitative and qualitative damage indices presented by other researchers were compared. A summary of these works was used to create quantitative and qualitative indexes of the joints.

#### 4.1.1. Hose et al.

Tables 9 and 10 present the results based on the flexural behavior of bridge members (cap beams and columns), as well as the damage and performance levels classified by Hose et al. (2000). Table 9 shows the damage levels, which range from capillary cracks at level I to permanent deformation and significant damage at level V. Table 10 shows the performance levels, which range

from cracking in level I to strength degradation in level V.

#### 4.1.2. Bahrani et al.

Bahrani et al. (2010) completed Hose et al. (2000) classifications, indices of performance and damage levels and classified the levels of performance for the joint region and flexural members (Tables 11 and 12). They also created qualitative classifications for damage and observed behavior at each of the five performance levels.

#### 4.1.3. Hassballa et al.

Table 13 summarizes Hasaballa et al. (2011) qualitative and quantitative definitions of joint damage (diagonal shear cracks to shear failure) in terms of the corresponding drift (1 percent to 5 percent).

#### 4.1.4. Vecchio et al.

Based on observations of damage in the joint region, Vecchio et al. (2014) classified joints into four performance levels. The damage characteristics for levels I through IV are shown in Table 14.

**Table 9.** Bridge damage assessment (Hose et al., 2000)

| Level | Damage classification     | Damage status  | Repair status   | Socio-economic status |
|-------|---------------------------|--|-----------------|-----------------------|
| I     | None                      | Barely visible cracking  | No repair       | Fully operational     |
| II    | Minor                     | Cracking   | Possible repair | Operational           |
| III   | Moderate                  | Open cracks; onset of spalling                                   | Minimum repair  | Life safety           |
| IV    | Major                     | Very wide cracks; extensive concrete spalling                    | Repair          | Near collapse         |
| V     | Local failure or collapse | Visible permanent deformation; buckling/rupture of reinforcement | Replacement     | Collapse              |

**Table 10.** Bridge performance assessment (Hose et al., 2000)

| Level | Performance level                   | Qualitative performance level  | Quantitative performance level  |
|-------|-------------------------------------|--|---|
| I     | Cracking                            | Onset of capillary cracks  | Barely visible cracking   |
| II    | Yielding                            | First longitudinal reinforcement yielding  | Crack width less than 1 mm  |
| III   | Onset of local mechanism            | Onset of inelastic deformation; onset of concrete spalling; development of diagonal cracks | Crack width of 1 to 2 mm; length of spalled region exceeds 1/10 of cross-section width  |
| IV    | Full development of local mechanism | Wide crack widths; spalling over full local mechanism region                               | Crack widths exceed 2 mm; Diagonal cracks exceed 2/3 of cross-section width; length of spalled region exceeds 1/2 cross-section width |
| V     | Strength degradation                | Main reinforcement buckling; Transverse reinforcement rupture; crushing of core concrete   | Crack width exceeds 2 mm in concrete core; Measurable dilation exceeds 5% of original member dimension                                |

**Table 11.** Damage based on performance level of joint (Bahrani et al., 2010)

| Level | Performance level                   | Qualitative description  | Quantitative description  |
|-------|-------------------------------------|--|---|
| I     | Cracking                            | Capillary cracks;<br>cold capillary cracks at joint;<br>onset of longitudinal reinforcement slip                       | Capillary cracks of less than 0.5 mm  |
| II    | Yielding                            | Concrete cold-joint crack opening  | Crack width of less than 1 mm   |
| III   | Onset of local mechanism            | Full-width cross-section crack; development of diagonal cracks; cap beam reinforcement slip; column reinforcement slip | Crack width of 1 to 2 mm;<br>concrete spalling of less than 1/10 of cross-section                                   |
| IV    | Full development of local mechanism | Concrete spalling; diagonal crack  | Crack width exceeds 2 mm;<br>spalling exceeds 1/2 of cross-section width; diagonal cracks over 2/3 of cross-section |
| V     | Strength degradation                | Severe column reinforcement slip; visible permanent deformation  | Crack of concrete core exceeds 2 mm   |

**Table 12.** Damage based on column performance levels (Bahrani et al., 2010)

| Level | Performance level                   | Qualitative performance level  | Quantitative performance level              |
|-------|-------------------------------------|--|---|
| I     | Cracking                            | Flexural capillary cracks  | Crack width of less than 0.5 mm             |
| II    | Yielding                            | Extension of flexural cracks   | Crack width of less than 1 mm               |
| III   | Onset of local mechanism            | Onset of concrete spalling; development of diagonal cracks                       | Crack width of 1 to 2 mm                    |
| IV    | Full development of local mechanism | Concrete spalling; diagonal cracks   | Spalling exceeds 1/2 of cross-section width |
| V     | Strength degradation                | Visible permanent deformation; buckling or rupture of longitudinal reinforcement | Crack in concrete core exceeds 2 mm         |

**Table 13.** Damage sequence by drift of joint (Hasaballa et al., 2011)

| Drift (%) | Damage                                |
|-----------|---------------------------------------|
| 1         | Diagonal shear cracks                 |
| 3         | Diagonal cracks of 2.6 mm in width    |
| 4         | Concrete spalling at bottom of joint  |
| 5         | Specimen failure due to shear failure |

**Table 14.** Performance criteria for joints from Vecchio et al. (2014)

| Level | Performance                   |
|-------|-------------------------------|
| I     | Beam bar yielding             |
| II    | Significant cracking of joint |
| III   | Joint shear mechanism         |
| IV    | Significant concrete spalling |

#### 4.1.5. Tukiari et al.

Tukiari et al. (2014) proposed five levels of performance for members, and Table 15 shows the qualitative descriptions for each level. In the current study, buckling of the reinforcement and collapse are considered separate items; however, Hose et al. (2000) combined them into one item.

#### 4.1.6. Truong et al.

Truong et al. (2017) calculated damage based on a 0.5 to 5% drift in the joint (Table 16). Truong et al. (2017) and Hasaballa et al. (2011) classified damage based on drift,

whereas others reported damage levels based on performance. At performance level 4, Bahrani et al. (2010) reported diagonal crack extension to more than two-thirds of the cross-section, whereas Truong et al. (2017) reported this damage at performance level 1. Full-width cracking did not occur in the current study, but it was observed by Bahrani et al. (2010). Using the findings of other researchers during experimental testing as well as those from the current study, a table was created in which the damage definitions were revised.



## 4.2. Performance of Specimens

### 4.2.1. Specimen SP-80

Figure 25 depicts the performance of the specimen SP-80 components in relation to drift. It can be seen that the damage trend and performance level for the joint were level III, level V for the cap beam, and level II for the column. This means that even if the joint is at level III, the column remains at level II. Despite the fact that the joint and cap beam have reached performance level V, the column has not been seriously damaged. This is in direct conflict with the seismic design criteria.

While studying the behavior of concrete bents in bridges, the performance of the joints has been the most important consideration. Figures 26 and 27 show the minimum drift for the SP-80 components

corresponding to the five performance levels. It can be seen that the joint and cap beam performed poorly, and these components were damaged much sooner than the column itself, which received little damage.

### 4.2.2. Specimen SP-90

Figure 28 depicts the damage trend and performance levels of the bent components in specimen SP-80. As can be seen, the cap beam reached level V, the joint reached level II, and the column reached only level II. This means that while the cap beam advanced to level IV, the column only advanced to level II. The cap beam experienced more damage than any other component, but the column did not sustain serious damage. This does not meet the seismic design criteria.

**Table 15.** Tukiari functional levels of flexural damage (Tukiari et al., 2014)

| Performance level   | Damage level   |
|---------------------|--|
| Operational         | No damage; fine cracks occur   |
| Immediate occupancy | Slight structural damage; initial spalling of concrete cover; entrance to building only to recover belongings                                    |
| Life safety         | Moderate structural damage; cracks in column and beam-column joint; buckling over reinforcement  |
| Collapse prevention | Large crack in structural elements; fracture of longitudinal bars; loss of stability of structure; structure near collapse and cannot be entered |
| Collapse prevention | Collapse or imminent danger of collapse  |

**Table 16.** Drift and sequence of damage to joint (Truong et al., 2017)

| Drift (%) | Damage observed   |
|-----------|---|
| 0.5       | Flexural cracks in beam   |
| 1         | Cracks propagating to neutral axis of beam  |
| 1.5       | Thin flexural cracks at beam-column interface that spread along beam length                                       |
| 3         | Onset of inclined cracks in joint panel zone; shear failure of joint panel zone as loading progresses             |
| 5         | Several thin vertical and horizontal cracks in joint panel zone; flexural cracks at widened beam-column interface |

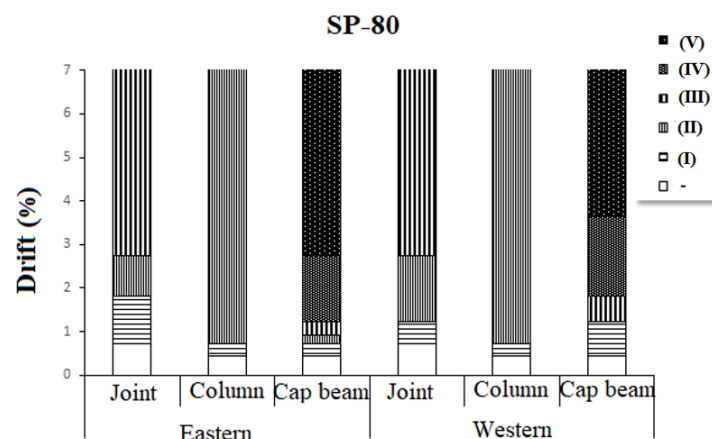


**Fig. 25.** Performance of components

Figures 29 and 30 represent the minimum drift values for each of the five performance levels. The joint and cap beam performance in specimen SP-90 can be seen to be completely rejected. The cap beam was damaged much earlier than the column,

and the column was only slightly damaged before the joint was damaged. The column eventually reached performance level II, and no damage matching levels III to V were observed. The joint performance, on the other hand, reached level IV.

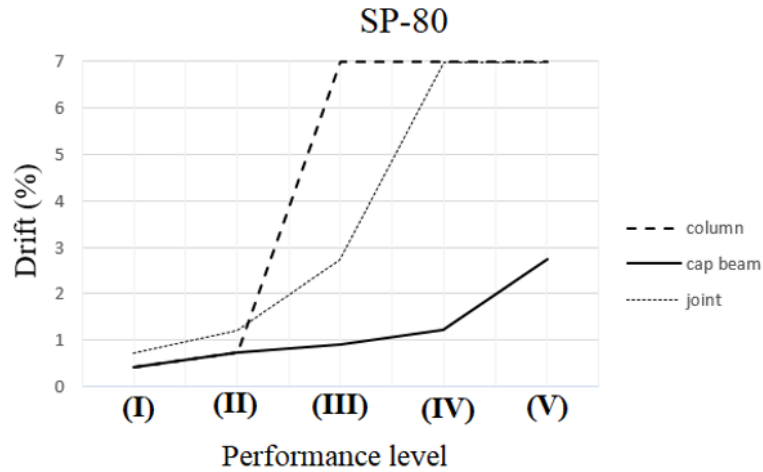


Fig. 26. Comparison of performance of components in SP-80



Fig. 27. Failure mode of SP-80

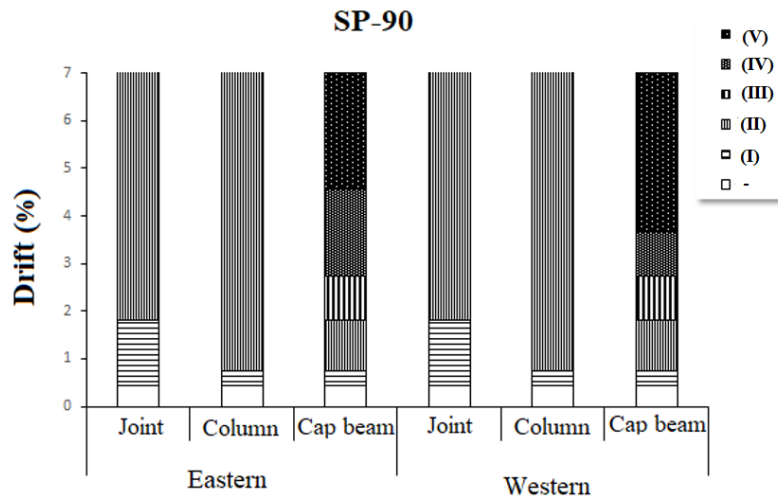


Fig. 28. Performance of components in SP-90

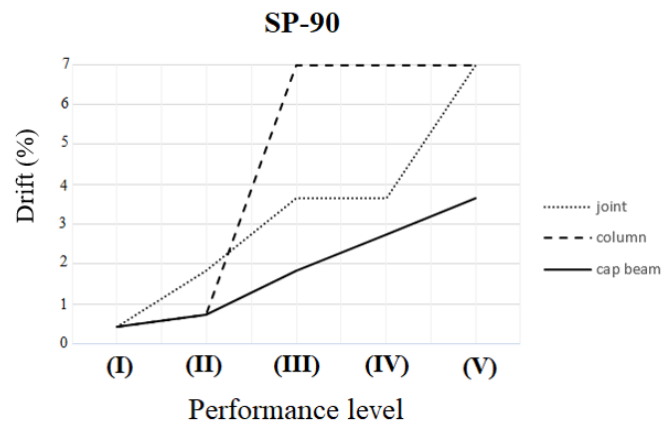


Fig. 29. Comparison of performance of components in SP-90

### 4.3. Energy Dissipation

The ability to dissipate energy is the most important parameter in structural seismic response. Figure 31 shows the increasing trend of cumulative dissipated energy by specimens. The specimen show relatively low drifts range at the end of test. Hysteresis curves represented little ability to absorbed and dissipate energy. Many reasons can be cited, including the defect of

structural details in older codes, the lack of a desirable failure mechanism, and the early occurrence of damage levels in the beams and connection region. A significant and significant result is the need to strengthen for the tested bents. As a result, more of the structure's capacity can be used for energy dissipation, and more deformation can occur.



Fig. 30. Failure mode of SP-90

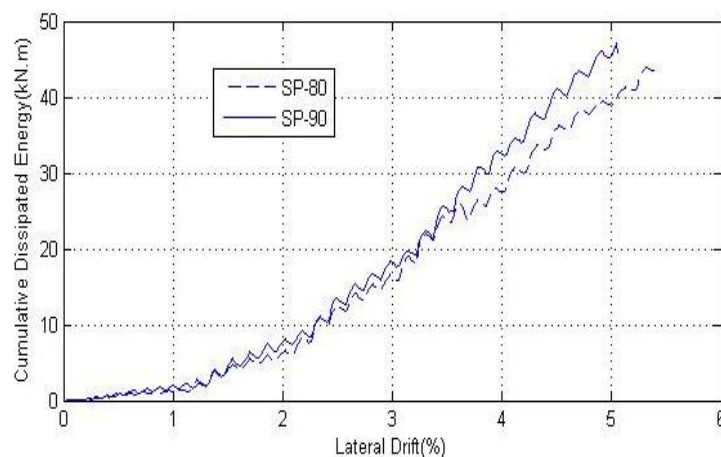


Fig. 31. Increase trend of cumulative dissipated energy

## 5. Conclusions

The present study performed an experimental evaluation and revised the performance level definitions for two-column concrete bridge bents with joints designed in the 1980s and 1990s. Based on the damage observed, qualitative and quantitative indexes for the performance levels have been presented. The performance of the bent's components was compared, and the following results were obtained:

- The minor change in the connection zone had little effect on bent strength and stiffness, as expected. The goal of increasing the number of stirrups in the joint region was to improve seismic behavior by changing the failure mechanism (moving the hinges to the top of the column). The observed damage revealed no positive change in the failure mechanism or movement of the flexural hinges to the column tops.
- Defining and developing quantitative and qualitative indices with appropriate performance levels for joints in concrete bridge bents is an important aspect of evaluating their seismic behavior and should be regarded as the first step in column strengthening.
- Damage assessment in the joint region revealed the problem of longitudinal column reinforcement embedded in the joint region. Cold capillary cracks were defects in performance level I and were classified as a sign of slippage and complete slippage by Bahrani et al. (2010) in performance levels III and V, respectively. This has not been addressed by Hose et al. (2000) and Tukiari et al. (2014) because they focused only on flexural members.
- The results showed that diagonal cracking was observed in the joint's first cycles and has been classified as performance level I. However, Hose et al. (2000) and Bahrani et al. (2010) based their observations on column damage, so they classified this observation as performance level III. The formation of diagonal cracks in the joint is included in performance level I.
- The findings revealed that the cold joint crack opening is a new qualitative definition in performance level I, with a quantitative definition of less than 1 mm.
- The findings revealed that vertical cracking in a joint that is accompanied by slipping of the column's longitudinal reinforcement, a cold joint crack width greater than 1 mm, and a crack width greater than 0.5 mm were all determinants of yielding. This level of performance is relative to the level of performance in the column.
- It was discovered that concrete crumbling of the joint's upper surface, slippage of the longitudinal reinforcement in the joint region, and permanent visible deformation of the joint due to loss of strength in the joint region all indicate performance level V in the columns. Fracture and buckling of the rebars are signs of this performance level.
- The joint and cap beam in SP-80 achieved performance levels III and V, respectively. However, the column's ultimate performance level was II. In SP-90, the beam and joint achieved performance levels V and II, respectively, despite the fact that the column's ultimate level was II.
- The results showed that the joint and cap beam were damaged before the columns in both experimental specimens. The columns did not meet their final performance levels, which contravened seismic design criteria.
- Test results revealed that the first cracks in the joint were diagonal cracks that occurred at lower drift values.
- Previous reports were based primarily on drift while, they were based on drift as well as performance level for each type of damage reported in the current study.
- Bahrani et al. (2010) reported cap beam and column reinforcement slippage. Only longitudinal column reinforcement

slippage due to strain penetration was observed in the current study.

## 6. Recommendations

Comparative behavioural evaluation of strengthened bridge pier bent with different spans can be studied. It is important that how bents behave in the similar lateral loading. According to the newer available bridge codes, to achieve the desired seismic behavior of concrete bent, different specimens can be tested and weaknesses should be evaluated.

## 7. References

- AASHTO. (2011). *AASHTO guide specifications for LRFD seismic bridge design*, AASHTO. Transportation Officials, Subcommittee on Bridges
- Abudallah Habib, I., Wan Mohtar, W.H.M., Muftah Shahot, K., El-shafie, A. and Abd Manan, T.S. (2020). "Bridge failure prevention: An overview of self-protected pier as flow altering countermeasures for scour protection", *Civil Engineering Infrastructures Journal*, 54(1), 1-22.
- Applied Technology Council (ATC24). (1992). "Guidelines for cyclic seismic testing of components of steel structures", Applied Technology Council, California.
- Bahrani, M.K., Vasseghi, A., Esmaeily, A. and Soltani, M. (2010). "Experimental study on seismic behavior of conventional concrete bridge bents", *Journal of Seismology and Earthquake Engineering*, 12(3), 107-118.
- Bahrani, M.K., Vasseghi, A., Nooralizadeh, A. and Zargaran, M. (2017). "Experimental and analytical study on the proposed retrofit method for concrete bent in ordinary highway bridges in Iran", *Journal of Bridge Engineering*, 22(6), 05017004.
- Billah, A.M., Alam, M.S. and Bhuiyan, M.R. (2012). "Fragility analysis of retrofitted multicolumn bridge bent subjected to near-fault and far-field ground motion", *Journal of Bridge Engineering*, 8(10), 992-1004.
- Deng, J., Liu, T., Xie, W., Wei Lu. (2015). "Study on repaired earthquake-damaged bridge piers under seismic load", *Advances in Materials Science and Engineering*, 2015, Article ID 295392, 10 pages.
- Ghassemieh, M., Ghodrati, S.M., Khanmohmmadi, M. and Baei, M. (2018). "A superelastic retrofitting method for mitigating the effects of seismic excitations on irregular bridges", *Civil Engineering Infrastructures Journal*, 51(1), 147-168.
- Hasaballa, M., El-ragaby, A., El-salakawy, E. (2011). "Seismic performance of exterior beam, Column joints reinforced with glass fibre reinforced polymer bars and stirrups", *Canadian Journal of Civil Engineering*, 38(10), 1092-1102.
- Hose, Y., Silva, P. and Seible, F. (2000). "Development of a performance evaluation database for concrete bridge components and systems under simulated seismic loads", *Earthquake Spectra*, 16(2), 413-442.
- Kaliluthin, A.K. and Kothandaraman, S. (2017). "Performance evaluation of exterior beam-column joint with core reinforcement technique subjected to reverse cyclic loading", *Arabian Journal for Science and Engineering*, 42(9), 2440-2443.
- Khanmohammadi, M., Abbasloo, A.A. and Valadi, E. (2016). "Enhancing shear strength of cap beam-column joints in existing multicolumn bent bridges using an innovative method", *Journal of Bridge Engineering*, 21(12), 04016086.
- Lowes, L.N. and Moehle, J.P. (1999). "Evaluation of retrofit of beam-column T-joints in older reinforced concrete bridge structures", *ACI Structural Journal*, 96(4), 519-532
- Naghavi, M., Rahnavard, R., Thomas, R.J. and Malekinejad, M. (2019). "Numerical evaluation of the hysteretic behavior of concentrically braced frames and buckling restrained brace frame systems", *Journal of Building Engineering*, 22, 415-428.
- Patel, P.A., Desai, A.K. and Desai, J.A. (2013). "Evaluation of RC and SFRC exterior beam-column joint under cyclic loading for reduction in lateral reinforcement of the joint region", *Magazine of Concrete Research*, 65(7), 405-414.
- Radkia, S., Gandomkar, F.A. and Rahnavard, R. (2018). "Seismic response of asymmetric sliding steel structure with considering soil-structure interaction effects", *Journal of Structural and Construction Engineering*, 6(3), 105-120.
- Radkia, S., Rahnavard, R. and Gandomkar, F.A. (2019). "Evaluation of the effect of different seismic isolators on the behavior of asymmetric steel sliding structures", *Journal of Structural and Construction Engineering*, 6(4), 213-230.
- Rahnavard, R. and Hassanipour, A. (2015). *Steel structures analysis using ABAQUS*, Academic Center for Education, Culture and Research, Publishing Organization of Kerman Branch, Kerman.
- Rahnavard, R., Hassanipour, A. and Mounesi, A. (2016). "Numerical study on important parameters of composite steel-concrete shear walls", *Journal of Constructional Steel Research*, 121, 441-456.
- Rahnavard, R., Hassanipour, A., Suleiman, M. and

- Mokhtari, A. (2017). "Evaluation on eccentrically braced frame with single and double shear panels", *Journal of Building Engineering*, 10, 13-25.
- Rahnavard, R., Naghavi, M., Aboudi, M. and Suleiman, M. (2018). "Investigating modeling approaches of buckling-restrained braces under cyclic loads", *Case Studies in Construction Materials*, 8, 476-488.
- Rahnavard, R., Taghikhajeh, M., Hassanipour, A. and Siahpolo, N. (2019). "Parametric study of seismic performance of steel bridges pier rehabilitated with composite connection", *Journal of Structural and Construction Engineering*, 6(1), 98-113.
- Rahnavard, R. and Thomas, R.J. (2019). "Numerical evaluation of steel-rubber isolator with single and multiple rubber cores", *Engineering Structures*, 198, 109532.
- Samadi, D., Taghaddos, H., Nili, M.H. and Noghabaei, M. (2021). "Development of a bridge maintenance system using bridge information modeling", *Civil Engineering Infrastructures Journal*, 54(2), 351-364.
- Truong, G.T., Hieu Dinh, N., Kim, J.C. and Choi, K.K. (2017). "Seismic performance of exterior RC beam-column joints retrofitted using various retrofit solutions", *International Journal of Concrete Structures and Materials*, 11(3), 415-433.
- Tukiar, M.A., Kay Dora, A.G. and Hamid, N.H. (2014). "Seismic performance and assessment of precast beam-column corner joint subject to reversible lateral cyclic loading", *Applied Mechanics and Materials*, 661(2014), 128-133.
- Vecchio, C.D., Di Ludovico, M., Balsamo, A., Prota, A., Manfredi, G. and Dolce, M. (2014). "Experimental investigation of exterior RC beam-column joints retrofitted with FRP systems", *Journal of Composites for Construction*, 18(4), 04014002.



This article is an open-access article distributed under the terms and conditions of the Creative Commons Attribution (CC-BY) license.